NASA Technical Memorandum 100567 NASA-TM-100567 19880017486

KINEMATICS OF HOOKE UNIVERSAL JOINT ROBOT WRISTS

William S. McKinney, Jr.

June 1988

NASA
National Aeronautics and
Space Administration

Langley Research Center
Hampton, Virginia 23665-5225

KINEMATICS OF HOOKE UNIVERSAL JOINT ROBOT WRISTS †

William S. McKinney, Jr.

SUMMARY

The singularity problem associated with wrist mechanisms commonly found on industrial manipulators can be alleviated by redesigning the wrist so that it functions as a three-axis gimbal system. This paper discusses the kinematics of gimbal robot wrists made of one and two Hooke universal joints. Derivations of the resolved rate motion control equations for the single and double Hooke universal joint wrists are presented using the three-axis gimbal system as a theoretical wrist model.

INTRODUCTION

Resolved rate motion control is a simple but effective method of controlling a robot arm in which an operator specifies the motion of the robot hand and a computer program resolves this commanded motion into individual robot joint motions. For a robot with six revolute joints, the commanded motion can often be separated into a translational component which is resolved into motions of the waist, shoulder, and elbow joints and a rotational component which is resolved into rotations about the three joint axes of the wrist (ref. 1). Unfortunately, many conventional industrial robot wrists cannot physically produce some commanded hand rotations. This condition occurs when two of the rotational axes of the wrist become aligned and appears as a singularity in the resolved rate control equations. References 2 and 3 discuss methods of coping with this singularity.

An alternative to using special methods to avoid the singularity of a conventional robot wrist is to redesign the wrist so that it operates in a manner similar to the three-axis gimbal system used in aircraft motion analysis (refs. 4 and 5). A three-axis gimbal wrist, when compared with conventional robot wrists, has a significantly increased singularity-free workspace and can improve robot performance in applications requiring dexterity similar to that of a human arm. Unfortunately, actually constructing a three-

† The mention herein of a tradename or a trademark of a commercial product does not consitiute any endorsement or recommendation for use by the Government.

axis gimbal wrist is a considerable challenge. References 6 and 7 discuss two wrist designs which do not produce purely rotational motions like a three-axis gimbal wrist, but do eliminate the singularity problem of the conventional robot wrist. Building a purely rotational wrist (which is desirable because it simplifies the resolved rate control equations for the robot) with a singularity-free workspace of at least a hemisphere continues to elude robot wrist designers.

The kinematics of a Hooke universal joint gimbal wrist design is discussed in this paper. If the workspace of the wrist can be limited to a cone with an included angle of about 90°, then a single Hooke joint can be used to build a true three-axis gimbal wrist. In order to expand the wrist workspace to a hemispherical surface, two Hooke joints must be used and translational velocities are introduced into the resolved rate control equations for the wrist. The purpose of this paper is to develop the kinematic resolved rate equations for gimbal-type wrists constructed from one and two Hooke universal joints. The analysis is presented using concepts from flight dynamics.

SYMBOLS

l	length of the intermediate shaft connecting two Hooke universal joints
$\vec{n}$, $\vec{o}$, $\vec{a}$, $\vec{u}$	columns 1, 2, 3, and 4, respectively, of a general transformation matrix
p, q, r	commanded rotational rates about X_H, Y_H, and Z_H, respectively
S_α, C_α	$\sin\alpha$ and $\cos\alpha$, respectively
$\mathrm{Rot}(A,\alpha)$	rotation transformation of an angle α about the A axis
$\mathrm{Trans}(A,u)$	translation transformation of a distance u along the A axis
$\dot{v}_{trans}$	translational velocity of the second joint of a double Hooke joint wrist
$(X_F\ Y_F\ Z_F)$	forearm axis system
$(X_H\ Y_H\ Z_H)$	hand axis system
$(X_{igd}\ Y_{igd}\ Z_{igd})$	inner gear drive axis system for the double Hooke joint wrist
$(X_{ogd}\ Y_{ogd}\ Z_{ogd})$	outer gear drive axis system for the double Hooke joint wrist
$(X_{Wi}\ Y_{Wi}\ Z_{Wi})$	the i^{th} wrist axis system

$Z_3,\ Z_4,\ Z_5$	rotational joint axes of a conventional robot wrist
β	angle between the driver shaft and the driven shaft of a Hooke universal joint
γ	angle of the driver shaft of a Hooke universal joint
$\theta_a,\ \psi_a$	actuator angles which produce Euler angles of θ and ψ
$\theta_4,\ \theta_5,\ \theta_6$	joint angles of a conventional robot wrist
$\phi,\ \theta,\ \psi$	Euler angles

A dot over a symbol indicates first derivative with respect to time. All vectors and transformations are expressed using the homogeneous transformation convention found in reference 8. Vectors are in lower case letters with arrows or are expressed by components. Coordinate system axes are in capital letters. For example, the vector $\vec{u}$ has coordinates $\{x_H\ y_H\ z_H\ 1\}^T$ when it is expressed in the $(X_H\ Y_H\ Z_H)$ axis system. The superscript T in the example means transpose. A caret ($\hat{}$) over a vector indicates that the vector is expressed in the robot's forearm coordinate system, which is considered fixed in this paper.

ANALYSIS

Figure 1 is a drawing of a typical industrial robot wrist. The rotational axes of the links of the wrist are the Z_3, Z_4, and Z_5 axes as shown. An operator commands rotational rates p, q, and r about the X_H, Y_H, and Z_H axes, respectively, of a right-handed axis system attached to the hand, and these rotational rates are resolved into rotational rates $\dot{\theta}_4$, $\dot{\theta}_5$, and $\dot{\theta}_6$ about the Z_3, Z_4, and Z_5 axes, respectively. The same wrist is shown in a singular configuration in figure 2, where the Z_3 and Z_5 axes are aligned and it is not physically possible for the wrist to instantaneously rotate in response to the commanded rotational rate p. A wrist design which avoids this problem is analyzed in this paper.

Three-Axis Gimbal Wrists

Reference 5 discusses the use of three-axis gimbal systems in real time flight simulations and how such systems could be applied to the resolved rate control of robot wrists. Figure 3 illustrates how a three-axis gimbal wrist is operated. The rotational rates p, q, and r are commanded about the X_H, Y_H, and Z_H axes of a coordi-

nate system attached to the hand of the robot. These commanded rates are resolved into the necessary gimbal angle rates $\dot{\phi}$, $\dot{\theta}$, and $\dot{\psi}$ about the X_W, Y_W, and Z_W axes of the wrist axis system. Gimbal angles are also known as Euler angles and will be called Euler angles for the rest of this text. The Euler angle convention used in this paper is described in detail in reference 4. The hand axis system is rotated by the ordered sequence of Euler angles: an angle ϕ about the X_W axis, an angle θ about the rotated Y_W axis, and an angle ψ about the rotated Z_W axis as shown in figure 3. The wrist axis system is referenced to an axis system fixed to the forearm of the robot (X_F Y_F Z_F). The orientation of the forearm axis system is the orientation of the wrist axis system at $\phi = \psi = \theta = 0°$. The hand, wrist, and forearm axis systems are drawn displaced in figure 3 for clarity, but are assumed to have a common origin. The well-known equations which relate the commanded rates in the hand axis system and the Euler angle rates are

$$\dot{\phi} = \frac{p\cos\psi - q\sin\psi}{\cos\theta} \tag{1}$$

$$\dot{\theta} = p\sin\psi + q\cos\psi \tag{2}$$

$$\dot{\psi} = r - \dot{\phi}\sin\theta \tag{3}$$

Equations (1), (2), and (3) are integrated to calculate ϕ, θ, and ψ. The transformation which relates a vector whose components are expressed in the forearm axis system (the unrotated wrist axis system) to the same vector expressed in the hand axis system is

$$\begin{Bmatrix} x_H \\ y_H \\ z_H \\ 1 \end{Bmatrix} = \begin{bmatrix} C_\theta C_\psi & (C_\phi S_\psi + S_\phi S_\theta C_\psi) & (S_\phi S_\psi - C_\phi S_\theta C_\psi) & 0 \\ -C_\theta S_\psi & (C_\phi C_\psi - S_\phi S_\theta S_\psi) & (S_\phi C_\psi + C_\phi S_\theta S_\psi) & 0 \\ S_\theta & -S_\phi C_\theta & C_\phi C_\theta & 0 \\ 0 & 0 & 0 & 1 \end{bmatrix} \begin{Bmatrix} x_F \\ y_F \\ z_F \\ 1 \end{Bmatrix} \tag{4}$$

where C_ψ means $\cos\psi$, S_θ means $\sin\theta$, etc. The inverse relation is found by transposing the matrix in equation (4).

Single Hooke Joint Wrists

The Hooke (or Cardan) joint is a mechanism which operates as a three-axis gimbal system. It consists of a driver shaft and a driven shaft connected by yokes to a cross.

The joint is often used as a coupling to transmit rotations between intersecting but misaligned shafts (ref. 9). A Hooke universal joint robot wrist is sketched in figure 4. The robot end effector is attached to the driven shaft of the joint. There are three actuators in the design: actuator 1 rotates the driver shaft; actuator 2 rotates the cross arm attached to the driver yoke; and actuator 3 rotates the driven yoke about its cross arm. The wrist and hand axis systems are assigned as follows.

The driver and driven shafts are aligned in the initial configuration of the wrist. The wrist axis system $(X_W\ Y_W\ Z_W)$ is located at the intersection of the cross with X_W directed along the driven shaft, Y_W directed along the cross arm connected to the driver shaft yoke, and Z_W directed along the cross arm connected to the yoke of the driven shaft to form a right-handed axis system. The forearm axis system $(X_F\ Y_F\ Z_F)$ is defined similarly when the shafts are aligned and is fixed in space. The hand axis system $(X_H\ Y_H\ Z_H)$ is defined in the same manner when the shafts are aligned, but is attached to the driven shaft of the joint, so that X_H always points in the direction of the driven shaft. With these axis system definitions, actuator 1 performs a rotation of ϕ about the X_W axis (a roll motion of the hand), actuator 2 performs a rotation of θ about the rotated Y_W axis (a pitch motion of the hand), and actuator 3 performs a rotation of ψ about the rotated Z_W axis (a yaw motion of the hand) in agreement with the Euler angle convention previously discussed. Therefore, equations (1), (2), and (3) are the resolved rate equations for actuators 1, 2, and 3, given commanded rotational rates p, q, and r in the hand axis system.

Although the single Hooke joint wrist has a singularity $\theta = \pm 90°$ (a condition known as gimbal lock), the Hooke joint has physical constraints that limit the useful range of motion of θ (and ψ) to values well below this singularity because of the high torques required at the driver shaft when the angle between the driver and driven shafts (labeled β in figure 4) approaches 90°. This is discussed in reference 9 where $q = r = 0$ and it is shown that the relationship between the commanded rotational rate p and the Euler angle rate $\dot{\phi}$ is

$$\frac{p}{\dot{\phi}} = \frac{\cos\beta}{1 - \sin^2\phi \sin^2\beta} \tag{5}$$

The angle β is of interest when calculating joint limits for the wrist and can be determined from ψ and θ as follows. Figure 5 traces the movement of the tip of the X_W axis as it is rotated by an angle θ about the Y_W axis to the point x' and an angle ψ about the rotated Z_W axis to the point x''. From the relations for right spherical triangles (ref.10) the relationship between β, θ, and ψ is

$$\cos\beta = \cos\theta \cos\psi \tag{6}$$

Equation (6) can be used to limit the workspace of the wrist to a cone with an included angle of 2β.

It is often more desirable for the wrist to have a singularity-free workspace of at least a hemisphere in teleoperated tasks. This is possible if the wrist is constructed from two Hooke joints and is discussed in the next section.

Double Hooke Joint Wrists

A double Hooke joint wrist is illustrated in figure 6. In the configuration shown, the rotational rate $\dot{\phi}_1$ of the driver shaft of the first joint is equal to the rotational rate $\dot{\phi}_2$ of the driven shaft of the second joint. However, it is very important to note that this relationship is true only if (A) the angle between the driver shaft of the first joint and the intermediate shaft, β_1, is equal to the angle between the intermediate shaft and driven shaft of the second joint, β_2, and (B) the yokes attached to the intermediate shaft lie in the same plane. This can be proved by noting that in the analysis in reference 9, the driver angle of the second joint (γ in figure 4), is 90° ahead of the output angle of the first joint, ϕ_1, because of the way the zero positions of the angles are defined.

Physically, the angles β_1 and β_2 can always be kept equal if the two joints are geared in such a manner that the actuators which perform the θ and ψ rotations at the first joint also force equal additional rotations of θ and ψ at the second joint through gearing between the joints. Reference 11 describes one implementation of this type of wrist. The forward kinematics for the double Hooke joint wrist is developed first, followed by a derivation of the rate equations.

The wrist and forearm axis systems for a double Hooke joint wrist are defined as in the previous section and are located at the first joint. For clarity, rotated wrist axis systems will be denoted by number as the forward kinematics is derived (e.g., the $(X_{W1}\ Y_{W1}\ Z_{W1})$ axis system is rotated into the $(X_{W2}\ Y_{W2}\ Z_{W2})$ axis system). The hand axis system is located at the center of the second joint and is attached to the driven shaft of the second joint. When $\beta_1 = \beta_2 = 0°$ the hand axis system, wrist axis system, and forearm axis system directions are the same. The hand axis system is translated away from the forearm axis system by the length l of the intermediate shaft.

The series of sketches in figure 7 show in detail the forward kinematics for this wrist. The initial position of the wrist is shown in figure 7(a). Starting from this position, actuator 1 rolls the wrist an angle of ϕ about the X_F axis, resulting in the $(X_{W1}\ Y_{W1}\ Z_{W1})$ axis system as shown in figure 7(b). A vector expressed in forearm coordinates is transformed to W_1 coordinates by

$$\begin{Bmatrix} x_{W1} \\ y_{W1} \\ z_{W1} \\ 1 \end{Bmatrix} = \mathrm{Rot}(X, \phi) \begin{Bmatrix} x_F \\ y_F \\ z_F \\ 1 \end{Bmatrix} \tag{7}$$

where

$$\mathrm{Rot}(X,\phi) = \begin{bmatrix} 1 & 0 & 0 & 0 \\ 0 & C_\phi & S_\phi & 0 \\ 0 & -S_\phi & C_\phi & 0 \\ 0 & 0 & 0 & 1 \end{bmatrix}$$

Next, actuator 2 rotates the cross arm connected to the driver yoke of the first joint an angle θ about the Y_{W1} axis resulting the in the $(X_{W2}\ Y_{W2}\ Z_{W2})$ axis system as shown in figure 7(c). A vector expressed in W_1 coordinates is transformed to W_2 coordinates by

$$\begin{Bmatrix} x_{W2} \\ y_{W2} \\ z_{W2} \\ 1 \end{Bmatrix} = \mathrm{Rot}(Y,\theta) \begin{Bmatrix} x_{W1} \\ y_{W1} \\ z_{W1} \\ 1 \end{Bmatrix} \tag{8}$$

where

$$\mathrm{Rot}(Y,\theta) = \begin{bmatrix} C_\theta & 0 & -S_\theta & 0 \\ 0 & 1 & 0 & 0 \\ S_\theta & 0 & C_\theta & 0 \\ 0 & 0 & 0 & 1 \end{bmatrix}$$

Then, actuator 3 rotates the driven yoke an angle ψ about the Z_{W2} axis resulting in the $(X_{W3}\ Y_{W3}\ Z_{W3})$ axis system as shown in figure 7(d). A vector expressed in W_2 coordinates is transformed to W_3 coordinates by

$$\begin{Bmatrix} x_{W3} \\ y_{W3} \\ z_{W3} \\ 1 \end{Bmatrix} = \mathrm{Rot}(Z,\psi) \begin{Bmatrix} x_{W2} \\ y_{W2} \\ z_{W2} \\ 1 \end{Bmatrix} \tag{9}$$

where

$$\mathrm{Rot}(Z,\psi) = \begin{bmatrix} C_\psi & S_\psi & 0 & 0 \\ -S_\psi & C_\psi & 0 & 0 \\ 0 & 0 & 1 & 0 \\ 0 & 0 & 0 & 1 \end{bmatrix}$$

Recall that it is assumed that gearing between the two Hooke joints produces additional θ and ψ rotations at the second joint. The next three transformations in this derivation describe the effect of the gearing between the joints and the fact that the hand axis system is located at the center of the second joint. There are only three actuators for this wrist. The following three transformations should not be confused as movements by more actuators.

The $(X_{W3}\ Y_{W3}\ Z_{W3})$ axis system is translated along the intermediate shaft (i.e., the X_{W3} axis) a distance l to the center of the second Hooke joint, resulting in the $(X_{W4}\ Y_{W4}\ Z_{W4})$ axis system as shown in figure 7(e). A vector expressed in W_3 coordinates is transformed to W_4 coordinates by

$$\begin{Bmatrix} x_{W4} \\ y_{W4} \\ z_{W4} \\ 1 \end{Bmatrix} = \mathrm{Trans}(X,l) \begin{Bmatrix} x_{W3} \\ y_{W3} \\ z_{W3} \\ 1 \end{Bmatrix} \tag{10}$$

where

$$\mathrm{Trans}(X,l) = \begin{bmatrix} 1 & 0 & 0 & -l \\ 0 & 1 & 0 & 0 \\ 0 & 0 & 1 & 0 \\ 0 & 0 & 0 & 1 \end{bmatrix}$$

Next, another rotation of ψ about the Z_{W4} axis takes place due to the gearing between the two joints, resulting in the $(X_{W5}\ Y_{W5}\ Z_{W5})$ axis system as shown in figure 7(f). A vector expressed in W_4 coordinates is transformed to W_5 coordinates by

$$\begin{Bmatrix} x_{W5} \\ y_{W5} \\ z_{W5} \\ 1 \end{Bmatrix} = \mathrm{Rot}(Z,\psi) \begin{Bmatrix} x_{W4} \\ y_{W4} \\ z_{W4} \\ 1 \end{Bmatrix} \tag{11}$$

Finally, also via the gearing, another rotation of θ about the Y_{W5} axis takes place resulting in the hand axis system as shown in figure 7(g). A vector expressed in W_5 coordinates is transformed to hand coordinates by

$$\begin{Bmatrix} x_H \\ y_H \\ z_H \\ 1 \end{Bmatrix} = \mathrm{Rot}(Y,\theta) \begin{Bmatrix} x_{W5} \\ y_{W5} \\ z_{W5} \\ 1 \end{Bmatrix} \tag{12}$$

Therefore, a vector expressed in forearm coordinates is transformed into hand coordinates by

$$X_F \xrightarrow{\phi} X_{W1} \xrightarrow{\theta} X_{W2} \xrightarrow{\psi} X_{W3} \xrightarrow{l} X_{W4} \xrightarrow{\psi} X_{W5} \xrightarrow{\theta} X_H$$

or,

$$\begin{Bmatrix} x_H \\ y_H \\ z_H \\ 1 \end{Bmatrix} = \mathrm{Rot}(Y,\theta)\mathrm{Rot}(Z,\psi)\mathrm{Trans}(X,l)\mathrm{Rot}(Z,\psi)\mathrm{Rot}(Y,\theta)\mathrm{Rot}(X,\phi) \begin{Bmatrix} x_F \\ y_F \\ z_F \\ 1 \end{Bmatrix}$$
$$= T_W \begin{Bmatrix} x_F \\ y_F \\ z_F \\ 1 \end{Bmatrix} \tag{13}$$

It requires a little algebra to symbolically calculate the complete wrist transformation T_W:

$$T_W = \begin{bmatrix} n_x & o_x & a_x & u_x \\ n_y & o_y & a_y & u_y \\ n_z & o_z & a_z & u_z \\ 0 & 0 & 0 & 1 \end{bmatrix} \tag{14}$$

where

$$\vec{n} = \begin{Bmatrix} 2C_\theta^2 C_\psi^2 - 1 \\ -2C_\theta S_\psi C_\psi \\ 2S_\theta C_\theta C_\psi^2 \end{Bmatrix}$$

$$\vec{o} = \begin{Bmatrix} 2C_\theta C_\psi (C_\phi S_\psi + S_\phi S_\theta C_\psi) \\ -2S_\psi (C_\phi S_\psi + S_\phi S_\theta C_\psi) + C_\phi \\ 2S_\theta C_\psi (C_\phi S_\psi + S_\phi S_\theta C_\psi) - S_\phi \end{Bmatrix}$$

$$\vec{a} = \begin{Bmatrix} 2C_\theta C_\psi (S_\phi S_\psi - C_\phi S_\theta C_\psi) \\ -2S_\psi (S_\phi S_\psi - C_\phi S_\theta C_\psi) + S_\phi \\ 2S_\theta C_\psi (S_\phi S_\psi - C_\phi S_\theta C_\psi) + C_\phi \end{Bmatrix}$$

$$\vec{u} = \begin{Bmatrix} -lC_\theta C_\psi \\ lS_\psi \\ -lS_\theta C_\psi \end{Bmatrix}$$

The inverse relation which transforms a vector in hand coordinates into the same vector in forearm coordinates is

$$\begin{Bmatrix} x_F \\ y_F \\ z_F \\ 1 \end{Bmatrix} = T_W^{-1} \begin{Bmatrix} x_H \\ y_H \\ z_H \\ 1 \end{Bmatrix} \tag{15}$$

where

$$T_W^{-1} = \begin{bmatrix} n_x & n_y & n_z & -\vec{u}\cdot\vec{n} \\ o_x & o_y & o_z & -\vec{u}\cdot\vec{o} \\ a_x & a_y & a_z & -\vec{u}\cdot\vec{a} \\ 0 & 0 & 0 & 1 \end{bmatrix}$$

and

$$\begin{Bmatrix} \vec{u}\cdot\vec{n} \\ \vec{u}\cdot\vec{o} \\ -\vec{u}\cdot\vec{a} \end{Bmatrix} \quad \begin{Bmatrix} lC_\theta C_\psi \\ l(C_\phi S_\psi + S_\phi S_\theta C_\psi) \\ l(S_\phi S_\psi - C_\phi S_\theta C_\psi) \end{Bmatrix}$$

The resolved rate equations are derived following a similar approach. Starting from the initial position, an angular rate $\dot{\phi}$ about X_F is transformed into the $(X_{W1}\ Y_{W1}\ Z_{W1})$ axis system:

$$\mathrm{Rot}(X,\phi) \begin{Bmatrix} \dot{\phi} \\ 0 \\ 0 \\ 1 \end{Bmatrix} = \begin{Bmatrix} \dot{\phi} \\ 0 \\ 0 \\ 1 \end{Bmatrix} \tag{16}$$

Next, an angluar rate $\dot{\theta}$ about the Y_{W1} axis is added to the angular velocity vector of equation (16) and the resulting vector is transformed into the $(X_{W2}\ Y_{W2}\ Z_{W2})$ axis system:

$$\mathrm{Rot}(Y,\theta) \begin{Bmatrix} \dot{\phi} \\ \dot{\theta} \\ 0 \\ 1 \end{Bmatrix} = \begin{Bmatrix} \dot{\phi}C_\theta \\ \dot{\theta} \\ \dot{\phi}S_\theta \\ 1 \end{Bmatrix} \tag{17}$$

Then, an angular rate $\dot{\psi}$ about the Z_{W2} axis is added to the angular velocity vector of equation (17) and the resulting vector is transformed into the $(X_{W3}\ Y_{W3}\ Z_{W3})$ axis system:

$$\mathrm{Rot}(Z,\psi)\begin{Bmatrix} \dot{\phi}C_\theta \\ \dot{\theta} \\ \dot{\phi}S_\theta + \dot{\psi} \\ 1 \end{Bmatrix} = \begin{Bmatrix} \dot{\phi}C_\theta C_\psi + \dot{\theta}S_\psi \\ -\dot{\phi}C_\theta S_\psi + \dot{\theta}C_\psi \\ \dot{\phi}S_\theta + \dot{\psi} \\ 1 \end{Bmatrix} \tag{18}$$

A translation occurs along the X_{W3} axis a distance l to the center of the second Hooke joint at this point in the forward kinematics. This does not affect the angular velocity vector in equation (18). However, the origin of the translated coordinate system has a translational velocity equal to the cross-product of the angular velocity vector and the position vector from the origin of the $(X_{W3}\ Y_{W3}\ Z_{W3})$ axis system to the origin of the $(X_{W4}\ Y_{W4}\ Z_{W4})$ axis system with both vectors expressed in $(X_{W3}\ Y_{W3}\ Z_{W3})$. Thus,

$$\begin{aligned} \vec{v}_{trans} &= \begin{Bmatrix} \dot{\phi}C_\theta C_\psi + \dot{\theta}S_\psi \\ -\dot{\phi}C_\theta S_\psi + \dot{\theta}C_\psi \\ \dot{\phi}S_\theta + \dot{\psi} \\ 1 \end{Bmatrix} \times \begin{Bmatrix} l \\ 0 \\ 0 \\ 1 \end{Bmatrix} \\ &= \begin{Bmatrix} 0 \\ l(\dot{\phi}S_\theta + \dot{\psi}) \\ l(\dot{\phi}C_\theta S_\psi - \dot{\theta}C_\psi) \\ 1 \end{Bmatrix} \end{aligned} \tag{19}$$

This velocity vector is expressed in forearm coordinates as

$$\begin{aligned} \hat{v}_{trans} &= [\mathrm{Rot}(Z,\psi)\mathrm{Rot}(Y,\theta)\mathrm{Rot}(X,\phi)]^{-1}\, \vec{v}_{trans} \\ &\begin{Bmatrix} -l(\dot{\theta}S_\theta C_\psi + \dot{\psi}C_\theta S_\psi) \\ l[\dot{\phi}(S_\phi S_\psi - C_\phi S_\theta C_\psi) + \dot{\theta}(S_\phi C_\theta C_\psi) + \dot{\psi}(C_\phi C_\psi - S_\phi S_\theta S_\psi)] \\ l[\dot{\phi}(C_\phi S_\psi + S_\phi S_\theta C_\psi) - \dot{\theta}(C_\phi C_\theta C_\psi) + \dot{\psi}(S_\phi C_\psi + C_\phi S_\theta S_\psi)] \\ 1 \end{Bmatrix} \end{aligned} \tag{20}$$

Equation (20) is integrated to obtain the position of the origin of the hand axis system expressed in forearm coordinates.

Since the translational velocity of the center of the second universal joint has been taken into account, only the angular velocity vector is considered for the rest of the derivation. Gearing in the wrist causes additional rotational rates $\dot{\psi}$ and $\dot{\theta}$ to occur at the second joint. Hence, $\dot{\psi}$ is added to the Z-component of the angular velocity vector in equation (18). The resulting vector is transformed into $(X_{W5}\ Y_{W5}\ Z_{W5})$ by

$$\mathrm{Rot}(Z,\psi)\begin{Bmatrix} \dot{\phi}C_\theta C_\psi + \dot{\theta}S_\psi \\ -\dot{\phi}C_\theta S_\psi + \dot{\theta}C_\psi \\ \dot{\phi}S_\theta + 2\dot{\psi} \\ 1 \end{Bmatrix} = \begin{Bmatrix} \dot{\phi}C_\theta C_{2\psi} + \dot{\theta}S_{2\psi} \\ -\dot{\phi}C_\theta S_{2\psi} + \dot{\theta}C_{2\psi} \\ \dot{\phi}S_\theta + 2\dot{\psi} \\ 1 \end{Bmatrix} \tag{21}$$

Finally, $\dot{\theta}$ is added to the Y-component of the angular velocity vector in equation (21), and the result is transformed into $(X_H\ Y_H\ Z_H)$ as

$$\mathrm{Rot}(Y,\theta)\begin{Bmatrix} \dot{\phi}C_\theta C_{2\psi} + \dot{\theta}S_{2\psi} \\ -\dot{\phi}C_\theta S_{2\psi} + \dot{\theta}(C_{2\psi}+1) \\ \dot{\phi}S_\theta + 2\dot{\psi} \\ 1 \end{Bmatrix} = \begin{Bmatrix} \dot{\phi}(C_\theta^2 C_{2\psi} - S_\theta^2) + \dot{\theta}C_\theta S_{2\psi} - 2\dot{\psi}S_\theta \\ -\dot{\phi}C_\theta S_{2\psi} + \dot{\theta}(C_{2\psi}+1) \\ \dot{\phi}S_\theta C_\theta(C_{2\psi}+1) + \dot{\theta}S_\theta S_{2\psi} + 2\dot{\psi}C_\theta \\ 1 \end{Bmatrix} \tag{22}$$

The final transformed angular rate vector in equation (22) must equal the commanded angular rates, p, q, and r. Therefore,

$$\begin{Bmatrix} p \\ q \\ r \\ 1 \end{Bmatrix} = \begin{bmatrix} C_\theta^2 C_{2\psi} - S_\theta^2 & C_\theta S_{2\psi} & -2S_\theta & 0 \\ -C_\theta S_{2\psi} & C_{2\psi}+1 & 0 & 0 \\ S_\theta C_\theta(C_{2\psi}+1) & S_\theta S_{2\psi} & 2C_\theta & 0 \\ 0 & 0 & 0 & 1 \end{bmatrix} \begin{Bmatrix} \dot{\phi} \\ \dot{\theta} \\ \dot{\psi} \\ 1 \end{Bmatrix} \tag{23}$$

From equation (23), the resolved rate equations for the double Hooke joint wrist are

$$\dot{\phi} = p - q\left(\frac{\tan\psi}{\cos\theta}\right) + r\tan\theta \tag{24}$$

$$\dot{\theta} = (p\cos\theta + r\sin\theta)\tan\psi + q\left(\frac{1 - 2\sin^2\psi}{2\cos^2\psi}\right) \tag{25}$$

$$\dot{\psi} = p\sin\theta + q\left(\frac{\tan\theta\tan\psi}{2}\right) + r\left(\frac{1 - 2\sin^2\theta}{2\cos\theta}\right) \tag{26}$$

The complete resolved rate equations for the double Hooke joint wrist are the rotational rate equations (24) to (26) and the translational rate equation (20). The rotational equations are singular for $\theta = \pm 90°$ and $\psi = \pm 90°$. But, as with the single Hooke joint wrist, θ and ψ should be limited to values well below these singularities due to the high torques required to roll the hand as β approaches 90°. Physically, the singularity at $\theta = \pm 90°$ means the first Hooke joint is in gimbal lock, and

the singularity at $\psi = \pm 90°$ means the second Hooke joint is in gimbal lock. For the wrist discussed in this section, the full range of ψ and θ should be limited to $\cos\psi\cos\theta \geq \cos 45°$. Since these angles are doubled at the second joint, the wrist works over a nearly hemispherical range and the resolved rate equations are never singular within its joint limits. Note that the curve traced by the tip of an end effector mounted to the driven shaft of the second joint is not circular. The distance from the tip of the end effector to the center of the first universal joint is not constant. For example, when $\psi = \theta = \phi = 0°$, the distance from the center of the first universal joint to the tip of the end effector is $l + e$ where e is the length of the end effector. When $\psi = 45°$ and $\theta = \phi = 0°$, this distance is shortened by $l/\sqrt{2}$. This should not be a significant problem for most applications.

The double Hooke joint wrist complicates the manipulator Jacobian when calculating joint rates for the entire robot arm. If the wrist is purely rotational, the upper right 3×3 matrix of the Jacobian for the robot is zero as discussed in reference 1. This means that the inverse kinematics can be explicitly derived for a robot with six degrees of freedom because the commanded translational velocities are a function of only the waist, shoulder, and elbow joints, i.e., the commanded translational velocity provides a set of three equations in three unknowns. The vector in equation (20) expressed in robot base or hand coordinates becomes part of the Jacobian of a robot with a double Hooke joint wrist. This increases the computational effort required to resolve the joint rates of the robot because the commanded translational motion of the hand is a function of all of the joint variables.

Actuators 2 and 3 of the Rosheim Omni-Wrist

One practical problem with both the single and double Hooke joint wrists discussed in the previous sections is that the axes driven by actuators 2 and 3 (the Y_W and Z_W axes) are rotated by actuator 1. Therefore, actuators 2 and 3 must either be carried by actuator 1 or some other provision must be made to transfer rotations by actuators 2 and 3 into rotations of θ and ψ. The Rosheim Omni-Wrist described in reference 11 presents one innovative solution to this problem.

The Omni-Wrist is shown in figure 8. The intermediate shaft of the two Hooke joints is the inner ring of a bearing whose outer rings are attached to inner and outer gear drives. Actuators 2 and 3 perform the θ and ψ rotations by rotating the outer and inner gear drives, respectively. The inner gear drive rotates in the plane of the paper (about the Y_F axis) and the outer gear drive rotates in and out of the paper (about the Z_F axis) as shown in figure 8. A cutaway section of the outer gear drive is shown in the figure. The position of the wrist is $\phi = 0°$, $\theta = 45°$, and $\psi = 0°$ as it appears in the figure. Rotations of the inner and outer gear drives uniquely determine the position of the outer rings of the bearing, and therefore determine the position of the intermediate shaft connecting the two Hooke joints. The position of the intermediate shaft is also uniquely determined by the Euler angles ϕ, θ, and ψ. The relationship

between the angles of actuators 2 and 3, denoted θ_a and ψ_a, respectively, and the Euler angles of the wrist are developed in this section.

Attach a coordinate system $(X_{igd}\ Y_{igd}\ Z_{igd})$ to the inner gear drive whose position at $\psi = \theta = \phi = 0^\circ$ coincides with $(X_F\ Y_F\ Z_F)$. Similarly, attach another coordinate system $(X_{ogd}\ Y_{ogd}\ Z_{ogd})$ to the outer gear drive. The inner gear rotates about the Z_{igd} axis (i.e., the Z_F axis) and the outer gear rotates about the Y_{ogd} axis (i.e., the Y_F axis). The outer rings of the bearing which are attached to the inner and outer gear drives are always coplanar with the plane defined by the Y_{igd} and Z_{ogd} axes. Since the intermediate shaft rides in the bearing, the axis of the intermediate shaft must therefore be perpendicular to the plane defined by Y_{igd} and Z_{ogd}. The axis of the intermediate shaft is the X_{W3} axis shown in figure 7(d). Therefore, the actuator angles θ_a and ψ_a are related to the Euler angles ϕ, θ, and ψ by

$$X_{W3} = \frac{Y_{igd} \times Z_{ogd}}{|Y_{igd} \times Z_{ogd}|} \tag{27}$$

The Y_{igd} axis expressed in forearm coordinates is

$$\hat{Y}_{igd} = \mathrm{Rot}(Z, \psi_a)^{-1} \begin{Bmatrix} 0 \\ 1 \\ 0 \\ 1 \end{Bmatrix} = \begin{Bmatrix} -S_{\psi_a} \\ C_{\psi_a} \\ 0 \\ 1 \end{Bmatrix} \tag{28}$$

The Z_{ogd} axis expressed in forearm coordinates is

$$\hat{Z}_{ogd} = \mathrm{Rot}(Y, \theta_a)^{-1} \begin{Bmatrix} 0 \\ 0 \\ 1 \\ 1 \end{Bmatrix} = \begin{Bmatrix} S_{\theta_a} \\ 0 \\ C_{\theta_a} \\ 1 \end{Bmatrix} \tag{29}$$

From equations (28) and (29), the unit vector formed by the cross product of Y_{igd} and Z_{ogd} expressed in forearm coordinates is

$$\frac{\hat{Y}_{igd} \times \hat{Z}_{ogd}}{\left|\hat{Y}_{igd} \times \hat{Z}_{ogd}\right|} = \left(\frac{1}{C^2_{\theta_a} + S^2_{\theta_a} C^2_{\psi_a}}\right) \begin{Bmatrix} C_{\theta_a} C_{\psi_a} \\ C_{\theta_a} S_{\psi_a} \\ -S_{\theta_a} C_{\psi_a} \\ 1 \end{Bmatrix} \tag{30}$$

The X_{W3} axis expressed in forearm coordinates is

$$\hat{X}_{W3} = [\mathrm{Rot}(Z,\psi)\mathrm{Rot}(Y,\theta)\mathrm{Rot}(X,\phi)]^{-1} \begin{Bmatrix} 1 \\ 0 \\ 0 \\ 1 \end{Bmatrix} = \begin{Bmatrix} C_\psi C_\theta \\ C_\phi S_\psi + S_\phi S_\theta C_\psi \\ S_\phi S_\psi - C_\phi S_\theta C_\psi \\ 1 \end{Bmatrix} \tag{31}$$

Substituting the results of equations (30) and (31) into equation (27) and equating vector components yields

$$\frac{C_{\theta_a} C_{\psi_a}}{C^2_{\theta_a} + S^2_{\theta_a} C^2_{\psi_a}} = C_\theta C_\psi \tag{32}$$

$$\frac{C_{\theta_a} S_{\psi_a}}{C^2_{\theta_a} + S^2_{\theta_a} C^2_{\psi_a}} = C_\phi S_\psi + S_\phi S_\theta C_\psi \tag{33}$$

$$\frac{-S_{\theta_a} C_{\psi_a}}{C^2_{\theta_a} + S^2_{\theta_a} C^2_{\psi_a}} = S_\phi S_\psi - C_\phi S_\theta C_\psi \tag{34}$$

The actuator angles for the Rosheim Omni-Wrist are determined by dividing equation (34) by equation (32) and equation (33) by equation (32). Thus,

$$\theta_a = \arctan\left[\frac{-S_\phi S_\psi + C_\phi S_\theta C_\psi}{C_\theta C_\psi}\right] \tag{35}$$

$$\psi_a = \arctan\left[\frac{C_\phi S_\psi + S_\phi S_\theta C_\psi}{C_\theta C_\psi}\right] \tag{36}$$

If the Rosheim Omni-Wrist is controlled by integrating equations (27) to (29) and position commands are sent to actuators 1, 2, and 3, then equations (35) and (36) can be used to calculate the proper commands to send to actuators 2 and 3.

CONCLUDING REMARKS

This paper has presented kinematic equations for gimbal-type robot wrists. The major benefit of the single Hooke joint wrist is that it is a purely rotational wrist which does not produce translational motions of the end effector. However, the single Hooke joint wrist has a rather limited range of motion due to the physical limitations of Hooke joints. On the other hand, the resolved rate equations for the double Hooke joint wrist

are still fairly simple and limits on end effector motion are also in the desired range. However, the computational effort required to control the robot is increased if the double Hooke joint wrist is used because of the translational velocities it produces in the end effector. Actuator implementations for single and double Hooke joint wrists have not been discussed in detail because of the large amount of information already in print on the subject and the variations in robot wrist designs of this type which exist (see refs. 12 and 13 and the similarities of the designs in refs. 6 and 7). The wrists in references 6 and 7 are also three axis wrists and are as effective in solving the singularity problems of conventional wrists as the Rosheim wrist. The Rosheim wrist may be well-suited for performing teleoperated assembly and repair applications because it can produce a true roll motion of the hand at any orientation using one actuator which is useful when performing tasks such as the insertion of screw fasteners.

REFERENCES

1. Barker, L. Keith: *Kinematic Equations for Resolved Rate Control of an Industrial Robot Arm*, NASA TM 85685, November 1983.

2. Barker, L. Keith: *Kinematic Control of a Robot With Degenerate Wrist*, NASA TP 2341, July 1984.

3. Paul, R. P., and C. N. Stephenson: "Kinematics of Robot Wrists," *The International Journal of Robotics Research*, 1983.

4. Thelander, J. A.: *Aircraft Motion Analysis*, FDL-TDR-64-70, U. S. Air Force, June, 1965.

5. Barker, L. Keith: *Theoretical Three- and Four-Axis Gimbal Robot Wrists*, NASA TP 2564, May 1986.

6. Milenkovic, Veljko: "New Nonsingular Robot Wrist Design," *Robots 11 Conference Proceedings RI/SME*, April 27-30, 1987, Chicago, Illinois.

7. Trevelyan, James P., et. al.: "ET: A Wrist Mechanism without Singular Positions," *The International Journal of Robotics Research*, Winter 1986.

8. Paul, R. P.: *Robot Manipulators: Mathematics, Programming, and Control*, MIT Press, 1981.

9. Shigley, Joseph Edward; and John Joseph Uicker, Jr.: *Theory of Mechanisms and Machines*, McGraw-Hill, 1980.

10. *CRC Standard Mathematical Tables*, 24th ed., CRC Press, 1976.

11. Rosheim, Mark E.: *Compact Robot Wrist Actuator*, United States Pat. 4,686,866, August 18, 1987.

12. Rosheim, Mark E.: "Singularity-Free Hollow Spray Painting Wrist," *Robots 11 Conference Proceedings RI/SME*, April 27-30, 1987, Chicago, Illinois.

13. Rosheim, Mark E.: "Four New Robot Wrist Actuators," *Robots 10 Conference Proceedings RI/SME*, April 20-24, 1986, Chicago, Illinois.

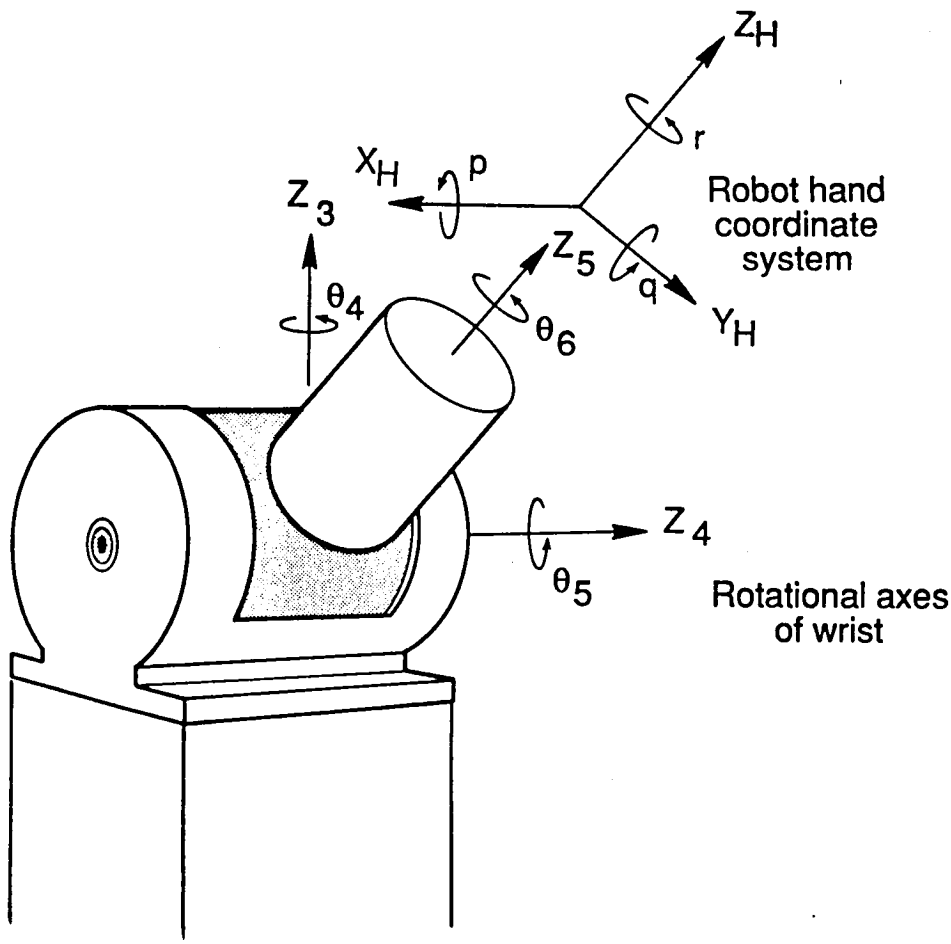

Figure 1. Conventional Robot Wrist.

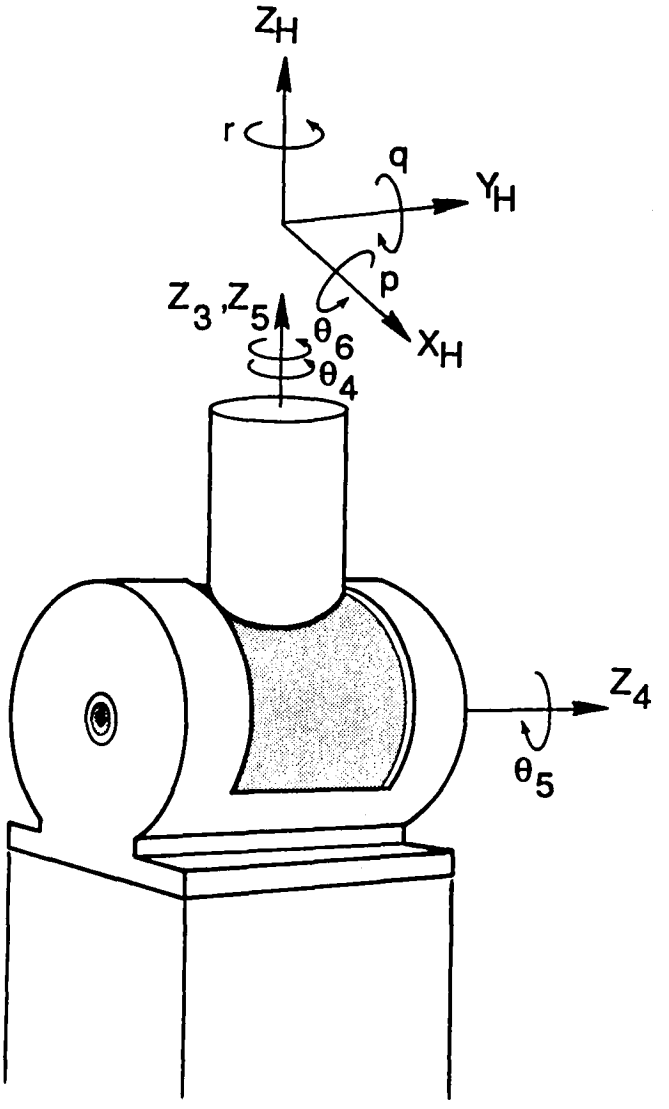

Figure 2. Singular Wrist Configuration.

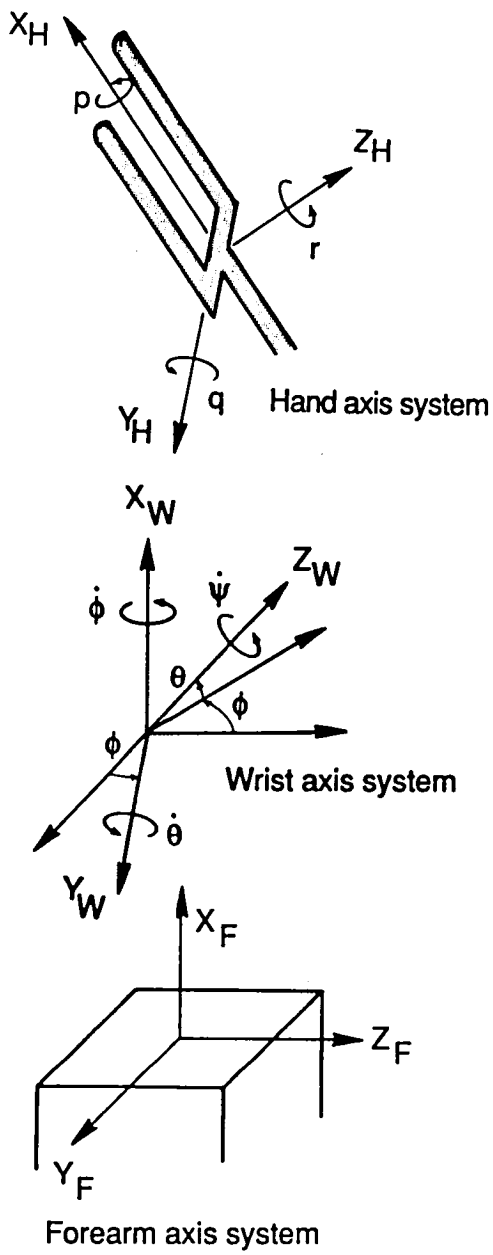

Figure 3. Three-Axis Gimbal Robot Wrist.

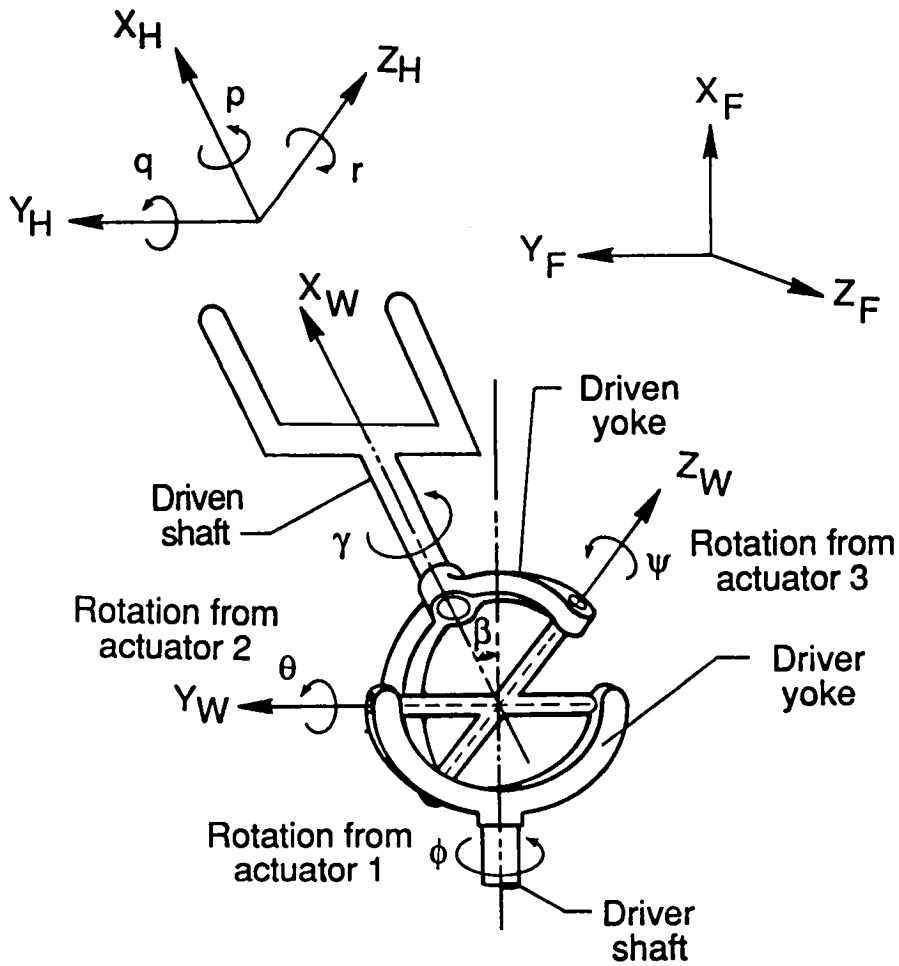

Figure 4. Hooke Universal Joint Robot Wrist.

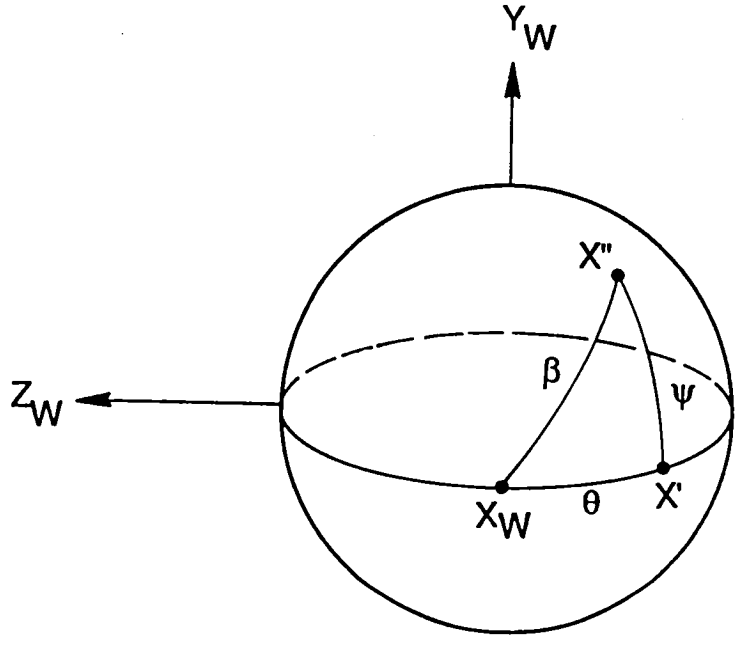

Figure 5. Relationship Between β, ψ, and θ.

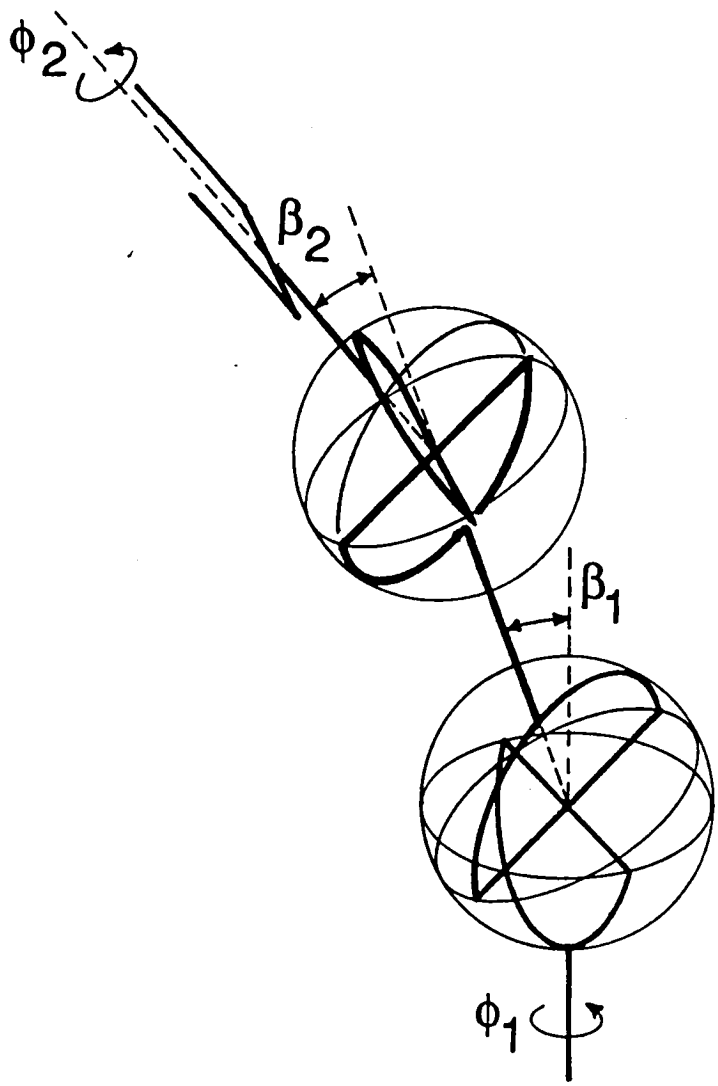

Figure 6. Double Hooke Joint Wrist.

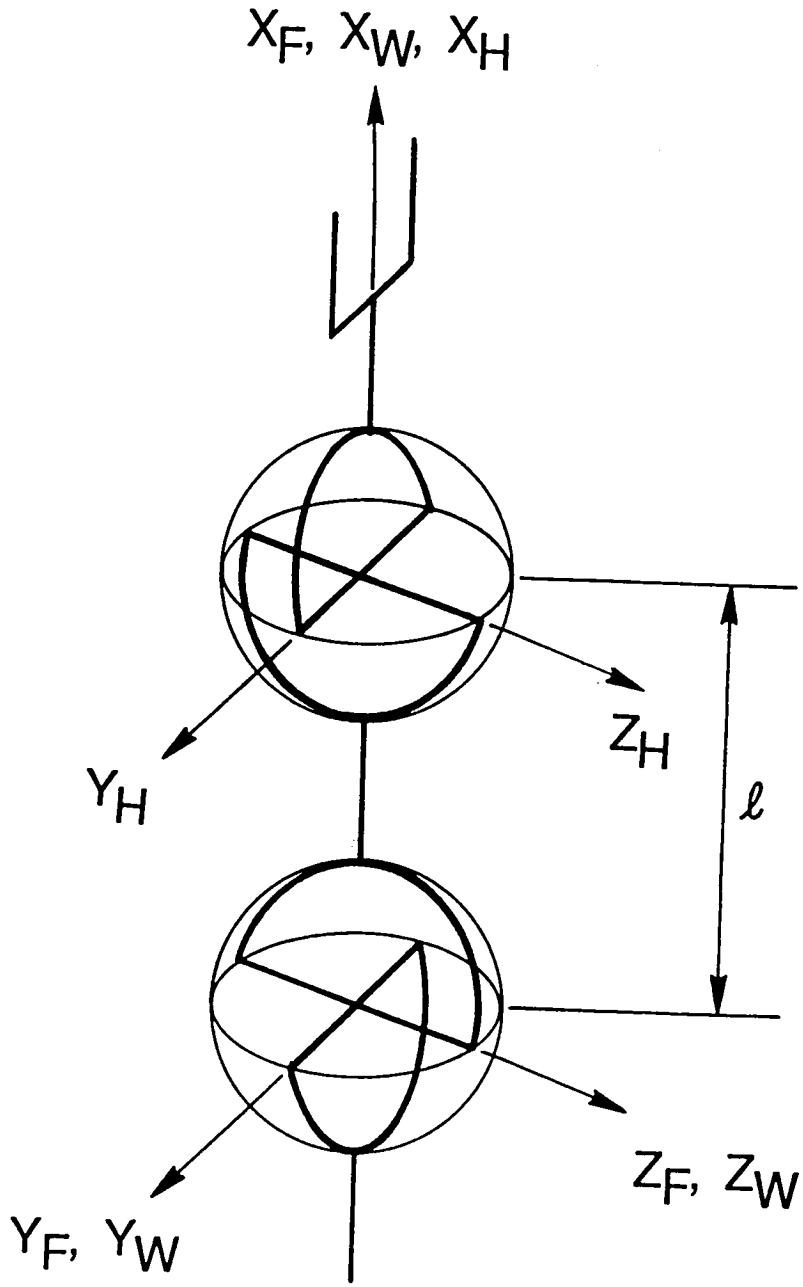

(a) Initial Position, $\beta_1 = \beta_2 = 0°$.

Figure 7. Forward Kinematics of the Double Hooke Joint Wrist.

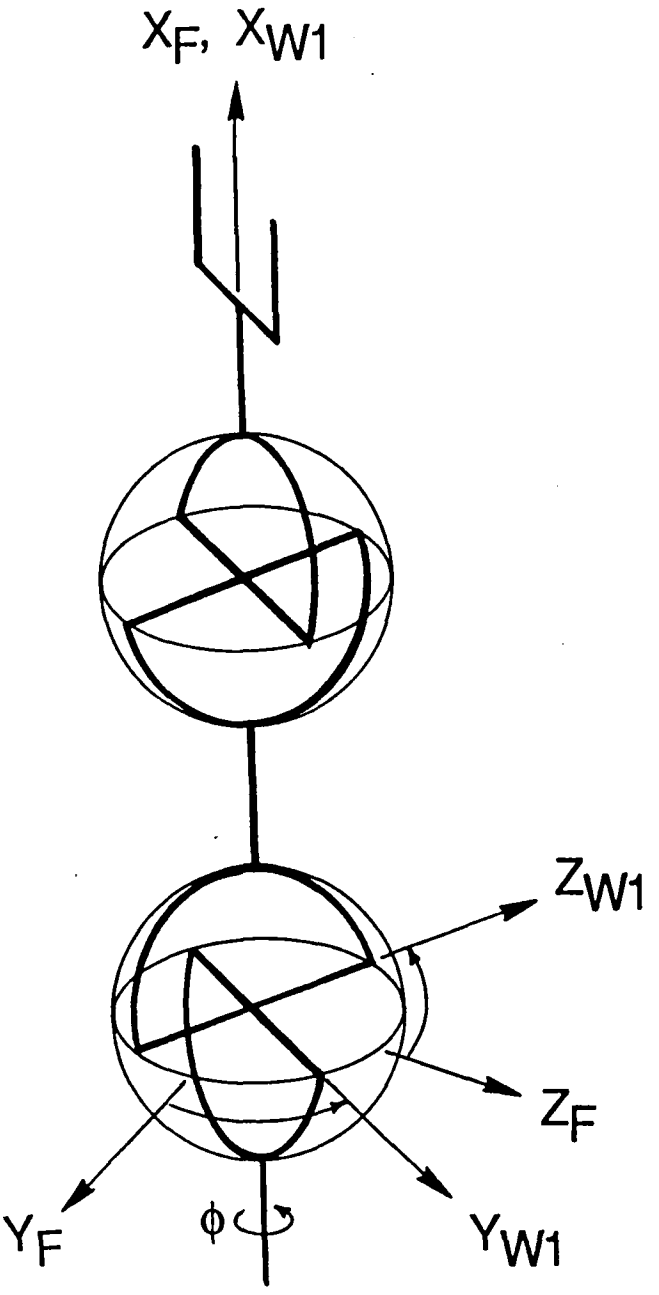

(b) $\mathrm{Rot}(X, \phi)$.

Figure 7. Continued.

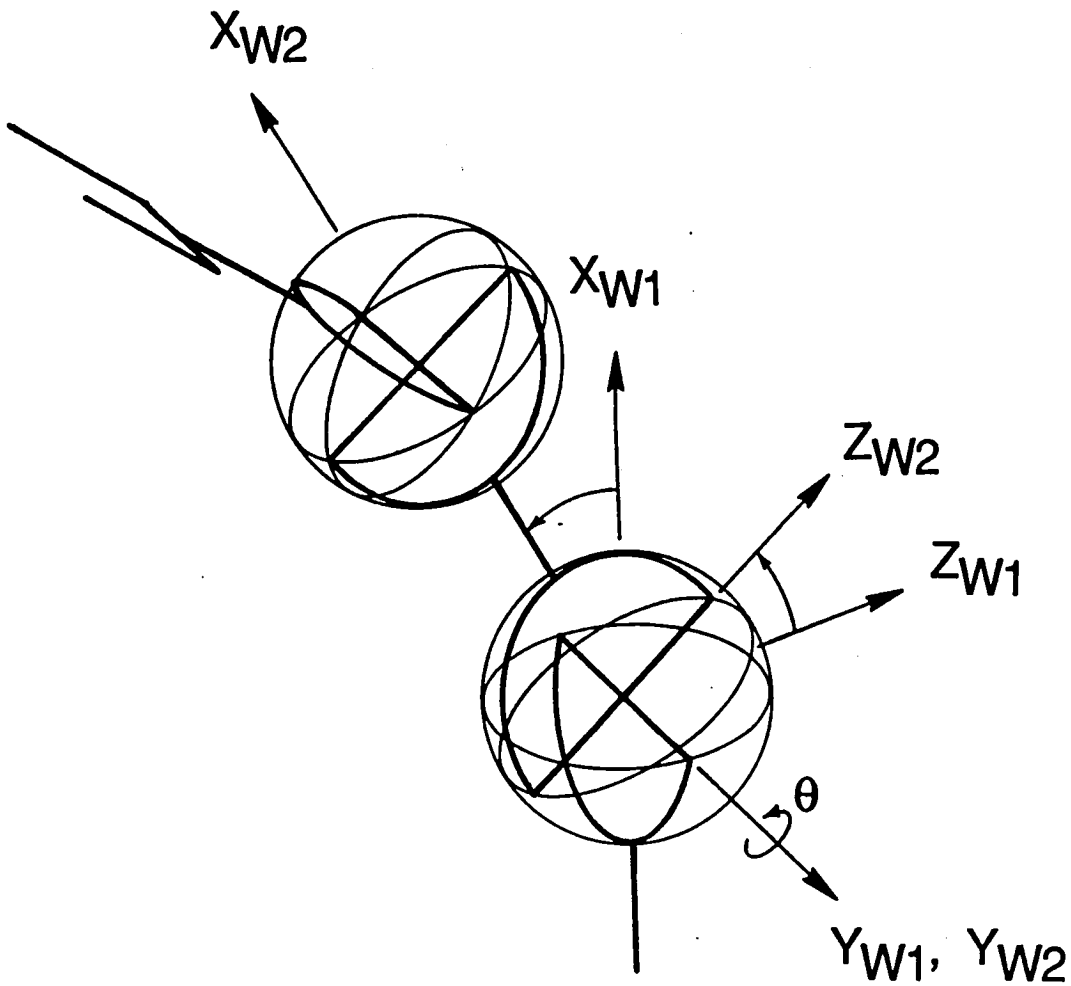

(c) Rot(Y, θ).

Figure 7. Continued.

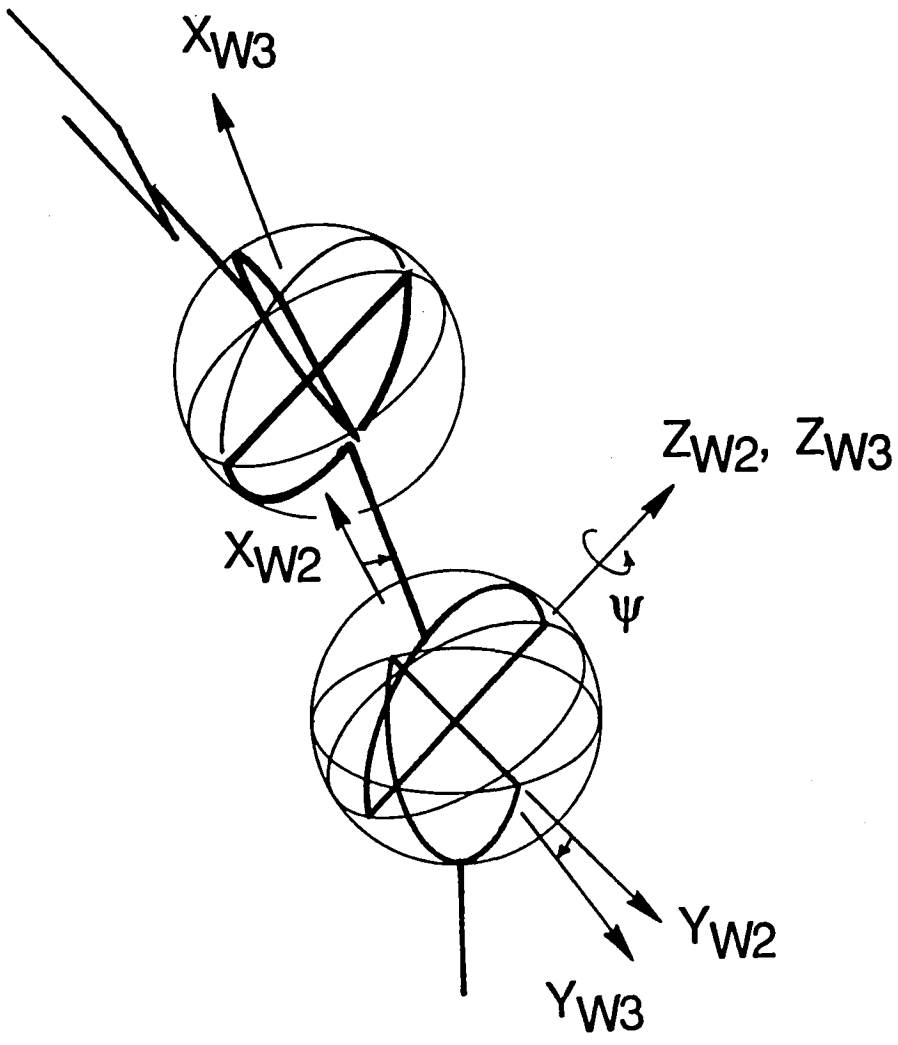

(d) Rot(Z, ψ).

Figure 7. Continued.

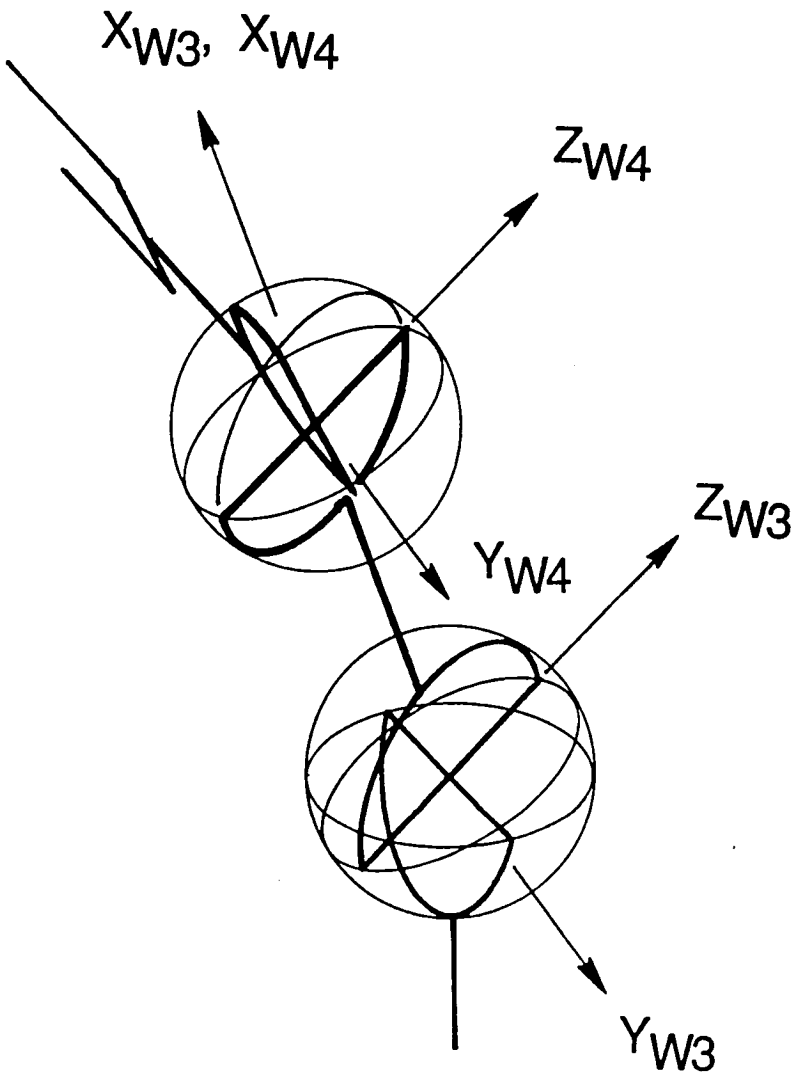

(e) Trans(X, l).

Figure 7. Continued.

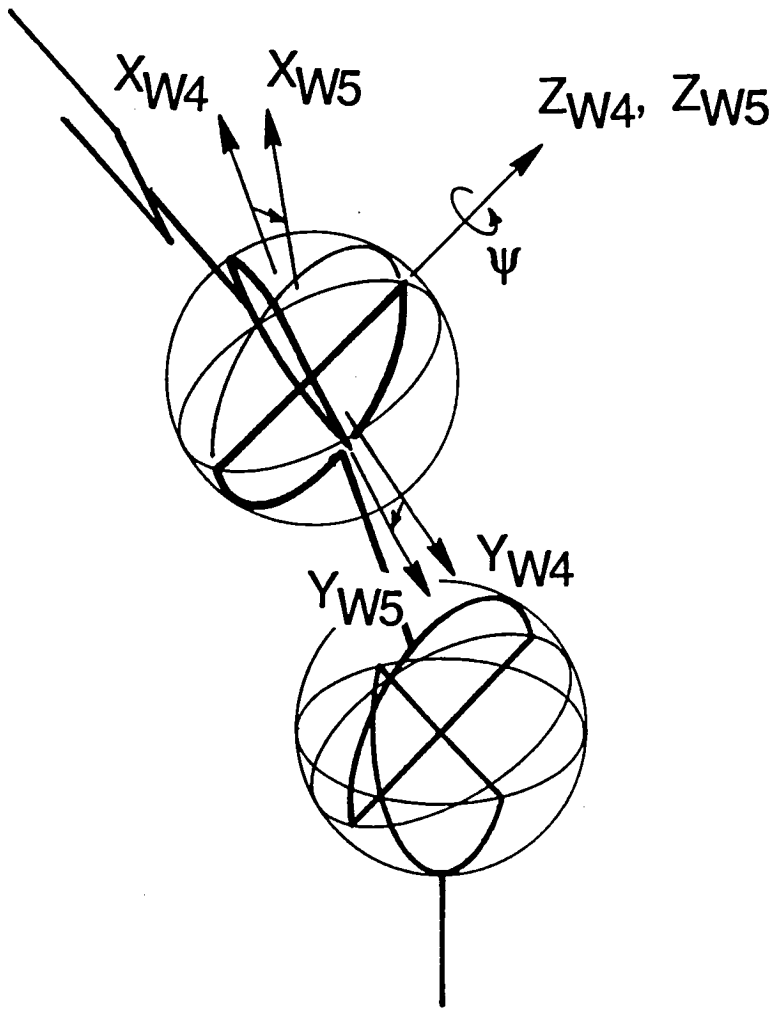

(f) $\mathrm{Rot}(Z, \psi)$.

Figure 7. Continued.

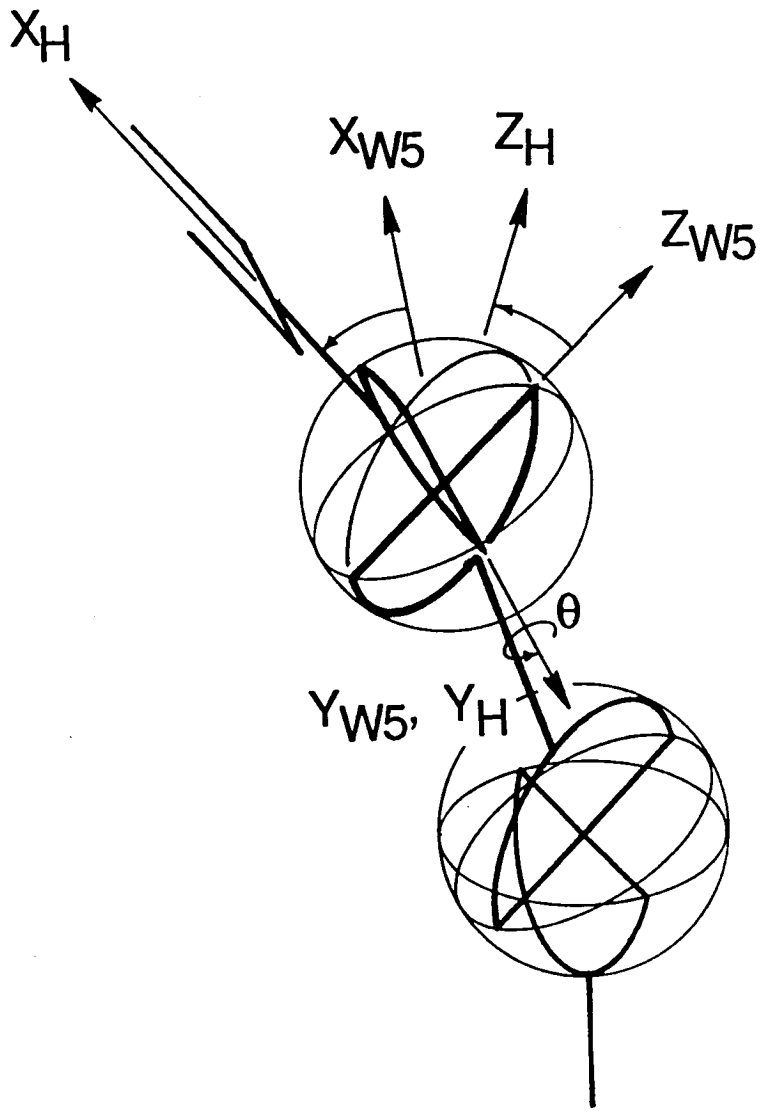

(g) Rot(Y, θ).

Figure 7. Continued.

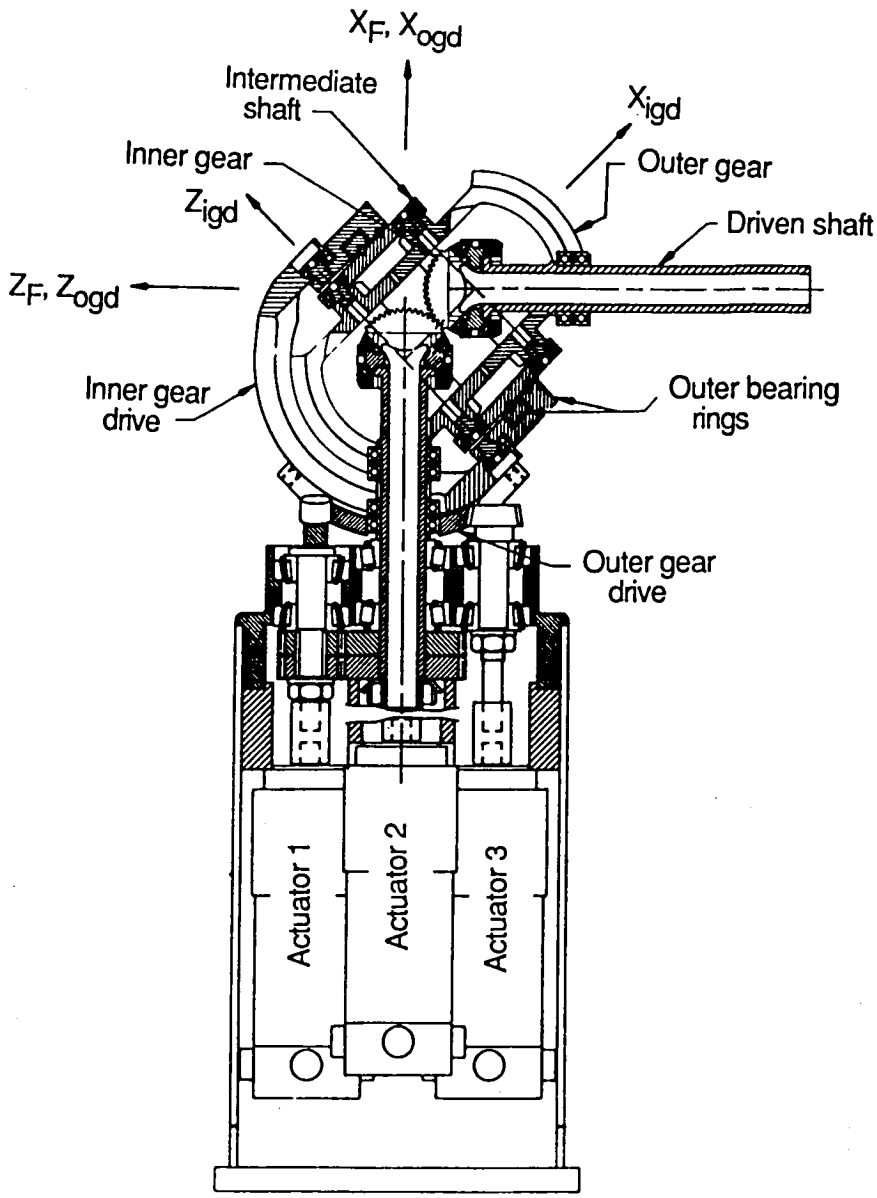

Figure 8. The Rosheim Omni Wrist.

NASA

Report Documentation Page

1. Report No.	2. Government Accession No.	3. Recipient's Catalog No.
NASA TM-100567		

4. Title and Subtitle	5. Report Date
Kinematics of Hooke Universal Joint Robot Wrists	June 1988
	6. Performing Organization Code

7. Author(s)	8. Performing Organization Report No.
William S. McKinney, Jr.	
	10. Work Unit No. 549-02-41-01

9. Performing Organization Name and Address	11. Contract or Grant No.
NASA Langley Research Center Hampton, VA 23665-5225	
	13. Type of Report and Period Covered: Technical Memorandum

12. Sponsoring Agency Name and Address	14. Sponsoring Agency Code
National Aeronautics and Space Administration Washington, DC 20546-0001	

15. Supplementary Notes

16. Abstract

The singularity problem associated with wrist mechanisms commonly found on industrial manipulators can be alleviated by redesigning the wrist so that it functions as a three-axis gimbal system. This paper discusses the kinematics of gimbal robot wrists made of one and two Hooke universal joints. Derivations of the resolved rate motion control equations for the single and double Hooke universal joint wrists are presented using the three-axis gimbal system as a theoretical wrist model.

17. Key Words (Suggested by Author(s))	18. Distribution Statement
Robot wrists Universal joints Robot kinematics Resolved rate control	Unclassified - Unlimited Subject Category 63

19. Security Classif. (of this report)	20. Security Classif. (of this page)	21. No. of pages	22. Price
Unclassified	Unclassified	32	A03